

The nonleptonic charmless decays of B_c meson

Wan-Li Ju,^{*} Tianhong Wang, Yue Jiang, Han Yuan, Guo-Li Wang^{†1}

¹*Department of Physics, Harbin Institute of Technology, Harbin, 150001, China*

Abstract

In this paper, with the framework of (p)NRQCD and SCET, the processes $B_c \rightarrow M_1 M_2$ are investigated. Here $M_{1(2)}$ denotes the light charmless meson, such as π , ρ , K or K^* . Based on the SCET power counting rules, the leading transition amplitudes are picked out, which include A_{wA}^2 , A_{wB}^2 , A_{wC}^2 , A_{wD}^2 and A_c^0 . From SCET, their factorization formulae are proven. Based on the obtained factorization formulae, in particular, the numerical calculation on A_{wB}^2 is performed.

^{*} wl_ju_hit@163.com

[†] gl_wang@hit.edu.cn

I. INTRODUCTION

Within the Standard Model, the B_c meson is the only pseudo-scalar meson formed by two different heavy flavor quarks. Due to its mass being under the BD threshold and the explicit flavors, B_c meson decays weakly but behaves stably via the strong and electromagnetic interactions. Its weak decay modes are expected to be rich, because the B_c meson contains two heavy quarks. Either can decay independent, or both of them annihilate to a virtual W boson.

In the recent decades, the decays of B_c meson have been widely studied. In this work, we lay stress on the two-body charmless processes $B_c \rightarrow M_1 M_2$. These charmless decays have particular features. First, they are not influenced by the penguin diagrams, which are expected to be sensitive to the new physics. Thus, they provide pure laboratories to examine the QCD effective methods. Second, they receive the contributions only from the annihilation amplitudes, which offer an ideal opportunity to study the annihilation effects singly.

In the paper [1], the nonleptonic charmless $B_c \rightarrow M_1 M_2$ decays have been calculated within the “QCD Factorization” approach (QCDF), while in Refs. [2, 3], these processes are calculated in the “perturbative QCD” (pQCD) schememethod. However, in this work, a sequence of effective field theories are employed to analysis the $B_c \rightarrow M_1 M_2$ transitions. Considering that the initial meson of the $B_c \rightarrow M_1 M_2$ transitions is B_c , which include two heavy quarks, we use the non-relativistic effective theory of QCD (NRQCD) [4, 5] to deal with them. Due to the relationship $M_{B_c} \gg M_{M_1} \sim M_{M_2}$, which makes that the final mesons are relativistically boosted and back-to-back move, we use soft collinear effective theory (SCET) [6–11] to describe these degrees of freedom (DOF). Under the SCET, it is convenient to explore the factorizations properties of the transition amplitudes.

This paper is organized as follows. In Sec. II, we introduce the theoretical details. We classify the transition amplitudes and focus on leading contributions. Within the framework of SCET, we prove the factorization formulae. Within Sec. III, according to the obtained factorization formulae, we calculate A_{wB}^2 and present the numerical results.

II. THEORETICAL DETAILS

In this section, we present the theoretical details. First of all, the general frameworks are shown and the transition amplitudes are classified into categories, A_w and A_c . Next, we pick out the leading contributions of A_w and A_c , respectively and prove the according factorization formulae.

A. Frameworks and Power Counting Rules

As to the $B_c \rightarrow M_1 M_2$ processes, there are three typical scales, m_b , $\sqrt{m_b \Lambda_H}$ and Λ_H . Λ_H is the typical hadronic scale. Conventionally, $\Lambda_H \sim 500$ MeV [11].

In order to describe the DOFs at scales $\sim m_b$, we use the full QCD and low-energy effective Hamiltonian [12], which is

$$H_W = \frac{2G_F}{\sqrt{2}} \sum_{q=d,s} V_{cb} V_{uq}^* (C_1 \bar{c}_L \gamma^\mu b_L \bar{q}_L \gamma_\mu u_L + C_2 \bar{c}_{L\beta} \gamma^\mu b_{L\alpha} \bar{q}_{L\alpha} \gamma_\mu u_{L\beta}) + h.c. \quad (1)$$

In Eq. (1), G_F denotes the Fermi coupling constant and $V_{q_1 q_2}$ s stand for the CKM matrix elements. $C_{1(2)}$ is the Wilson coefficients. μ represents the Lorentz index, while $\alpha(\beta)$ is the color index.

For investigating the $\sqrt{m_b \Lambda_H}$ fluctuations, we need to integrate out the hard modes $\sim m_b$, obtaining several transition currents J^I and the intermediate effective theory SECT_I+NRQCD. Within SECT_I [6–9], there are three kinds of DOFs [7]: 1) the n -collinear quarks ξ_n^I and gluons A_n^I with the momentum scaling $p_c = (n \cdot p_c, \bar{n} \cdot p_c, p_{c\perp}) \sim m_b(\lambda^2, 1, \lambda)$; 2) the \bar{n} -collinear quarks $\xi_{\bar{n}}^I$ and gluons $A_{\bar{n}}^I$ with the momenta $p_{\bar{c}} \sim m_b(1, \lambda^2, \lambda)$; 3) the ultra-soft quarks ξ_{us}^I and gluons A_{us}^I with $p_{us} \sim m_b(\lambda^2, \lambda^2, \lambda^2)$. $\lambda = \sqrt{\Lambda_H/m_b}$ is the expansion parameter. The power counting rules for these SECT_I fields [7] are summarized in Table. I.

Within NRQCD [4, 5], there are four typical fields [13]: 1) the Pauli spinor quark field $\psi(\chi)$ with momentum $p_{\varphi(\chi)}^{\text{NR}} = (E, \vec{p}) \sim (\frac{|\vec{q}_{B_c}|}{M_{B_c}}, \vec{q}_{B_c})$; 2) the potential gluon field A_p^{NR} with momentum $p_p^{\text{NR}} \sim (\frac{|\vec{q}_{B_c}|}{M_{B_c}}, \vec{q}_{B_c})$; 3) the soft gluon field A_s^{NR} with momentum $p_s^{\text{NR}} \sim (|\vec{q}_{B_c}|, \vec{q}_{B_c})$; 4) the ultra-soft gluon field A_{us}^{NR} with momentum $p_{us}^{\text{NR}} \sim (\frac{|\vec{q}_{B_c}|}{M_{B_c}}, \frac{\vec{q}_{B_c}}{M_{B_c}})$. \vec{q}_{B_c} is the relative momentum between the quark and the anti-quark of the B_c meson. According the recent analysis [14], we take $\vec{q}_{B_c}^2 \sim 1 \text{ GeV}^2$. Therefore, numerically, we have $\sqrt{(p_s^{\text{NR}})^2} \sim \sqrt{(p_s^{\text{NR}})^2} \sim$

TABLE I: Power counting Rules for the SECT_I and SECT_{II} fields [7, 9].

Fields	Field Scaling	Fields	Field Scaling
$\xi_{n(\bar{n})}^I$	λ	$\xi_{n(\bar{n})}^{II}$	η
ξ_{us}^I	λ^3	ξ_s^{II}	$\eta^{3/2}$
$(A_n^I \cdot n, A_n^I \cdot \bar{n}, A_{n\perp}^I)$	$(\lambda^2, 1, \lambda)$	$(A_n^{II} \cdot n, A_n^{II} \cdot \bar{n}, A_{n\perp}^{II})$	$(\eta^2, 1, \eta)$
$(A_{\bar{n}}^I \cdot n, A_{\bar{n}}^I \cdot \bar{n}, A_{\bar{n}\perp}^I)$	$(1, \lambda^2, \lambda)$	$(A_{\bar{n}}^{II} \cdot n, A_{\bar{n}}^{II} \cdot \bar{n}, A_{\bar{n}\perp}^{II})$	$(1, \eta^2, \eta)$
A_{us}^I	λ^2	A_s^{II}	η

$\sqrt{m_b \Lambda_H}$.

As to the transition currents J^I s, they fall into two categories: 1) the weak flavor transition currents J_w^I s, which are induced by H_W ; 2) the QCD currents J_c^I s, which are caused by the pure QCD interactions and obtained by integrating out the hard ($\sim m_b$) QCD interactions. According to the number of J_c^I s, it is convenient to classify the transition amplitudes into two types, A_w s which are induced by no J_c^I s, and A_c s those are mediated by at least one J_c^I s.

For describing the DOFs $\sim \Lambda_H$, the intermediate fluctuations $\sim \sqrt{m_b \Lambda_H}$ are integrated out. Then, the transition currents J^{II} and final effective theory pNRQCD + SECT_{II} are matched onto, corresponding to the Λ_H momentum modes. In the framework of pNRQCD [5], the momentum modes p_s^{NR} and $p_{\bar{s}}^{\text{NR}}$ are integrated out, leaving only the ultra-soft gluon A_{us}^{NR} and the Pauli spinor quark field $\psi(\chi)$. In SECT_{II} [10, 11], similar to the case of SECT_I, there are also three typical momentum regions: 1) the n -collinear quarks ξ_n^{II} and gluons A_n^{II} with $p_c \sim m_b(\eta^2, 1, \eta)$; 2) the \bar{n} -collinear quarks $\xi_{\bar{n}}^{II}$ and gluons $A_{\bar{n}}^{II}$ with $p_{\bar{c}} \sim m_b(1, \eta^2, \eta)$; 3) the soft quarks ξ_s^{II} and gluons A_s^{II} with $p_s \sim m_b(\eta, \eta, \eta)$. Here $\eta = \lambda^2 = \Lambda_H/m_b$ is the expansion parameter. The field scalings for these SECT_{II} fields [7] are also listed in Table. I.

B. The Leading contributions of A_w

In this part, we pick out the leading contributions of A_w . At the scale $\sim \sqrt{m_b \Lambda_H}$, A_w is induced by J_w^I s and the SCET_I Lagrangian \mathcal{L}_c and \mathcal{L}_{us} . Here we have $\mathcal{L}_c = \mathcal{L}_{\xi\xi}^0 + \mathcal{L}_{\xi\xi}^1 + \mathcal{L}_{\xi\xi}^2 + \mathcal{L}_{\xi q}^1 + \mathcal{L}_{\xi q}^{2a} + \mathcal{L}_{\xi q}^{2b} + \mathcal{L}_{cg}^0 + \mathcal{L}_{cg}^1 + \mathcal{L}_{cg}^2$. The explicit forms of these SCET_I Lagrangian can

be found in Ref. [11]. The relevant J_w^I s in this work are

$$\begin{aligned}
J_w^0 &= \int d\omega_2 d\omega_4 \left[C_w^{01}(\omega_2, \omega_4) \left(\chi_{\bar{c}}^\dagger \Gamma_A^{01} \psi_b \right) (\bar{q}'_{\bar{n}, \omega_2} \Gamma_B^{01} q_{n, \omega_4}) + C_w^{02} \left(\chi_{\bar{c}, \beta}^\dagger \Gamma_A^{02} \psi_{b, \alpha} \right) (\bar{q}'_{\bar{n}, \omega_2, \alpha} \Gamma_B^{02} q_{n, \omega_4, \beta}) \right], \\
J_w^1 &= \int d\omega d\omega_2 d\omega_3 C_w^1(\omega, \omega_2, \omega_3) \left(\chi_{\bar{c}}^\dagger \Gamma_\mu^1 B_{n, \omega}^{\perp \mu} \psi_b \right) (\bar{q}'_{\bar{n}, \omega_2} \Gamma_{\bar{n}} q_{\bar{n}, \omega_3}), \\
J_w^{2A} &= \int d\omega_1 d\omega_2 d\omega_3 d\omega_4 C_w^{2A}(\omega_1, \omega_2, \omega_3, \omega_4) \left(\chi_{\bar{c}}^\dagger \Gamma_{\mu\nu}^{2A} \psi_b \right) (\bar{q}'_{\bar{n}, \omega_2} \Gamma_{\bar{n}} q_{\bar{n}, \omega_3}) \text{Tr} [B_{n, \omega_1}^{\perp \mu} B_{n, \omega_4}^{\perp \nu}], \\
J_w^{2B} &= \int d\omega_1 d\omega_2 d\omega_3 d\omega_4 C_w^{2B}(\omega_1, \omega_2, \omega_3, \omega_4) \left(\chi_{\bar{c}}^\dagger \Gamma^{2B} \psi_b \right) (\bar{q}'_{\bar{n}, \omega_2} \Gamma_{\bar{n}} q_{\bar{n}, \omega_3}) (\bar{q}'_{n, \omega_1} \Gamma_n q_{n, \omega_4}),
\end{aligned} \tag{2}$$

where $\chi_{\bar{c}}$ and ψ_b are the Pauli spinor fields corresponding to the \bar{c} and b quarks, respectively. q_{n, ω_i} s are defined as $q_{n, \omega_i} \equiv [\delta(\bar{n} \cdot \mathcal{P} - \omega_i) W_n^\dagger \xi_n^I]$ [15]. \mathcal{P} is the operator picking out the large label momenta. W_n is the conventional Wilson line $W_n[\bar{n} \cdot A_n^I]$ after extracting the phase exponent $e^{-i\mathcal{P} \cdot x}$. ξ_n^I is the n -collinear field in SCET_I, as introduced in Sec. II A.

In Eq. (2), $B_{n, \omega}^\perp$ is also introduced, which is defined as $B_{n, \omega}^\perp \equiv [B_n^\perp \delta(\bar{n} \cdot \mathcal{P}^\dagger - \omega)]$. Here we have [16]

$$B_n^{\perp \mu} = \frac{1}{g} \left[\frac{1}{\bar{n} \cdot \mathcal{P}} W_n^\dagger [i\bar{n} \cdot D_n, iD_n^{\perp \mu}] W_n \right], \tag{3}$$

where $i\bar{n} \cdot D_n = \bar{n} \cdot \mathcal{P} + g\bar{n} \cdot A_n^I$ and $iD_n^\perp = \mathcal{P}^\perp + gA_n^{\perp I}$. Using the building operators q_{n, ω_i} and $B_{n, \omega}^\perp$ to construct the currents is quite convenient, because these building blocks are invariant under the collinear-gauge transformations [9].

Within SCET_I, the scaling of A_w can be expressed as $\lambda^{N_J + N_{\mathcal{L}}}(N_J, N_{\mathcal{L}} \geq 0)$. λ^{N_J} is the power counting for J_w^I s. For instance, λ^1 corresponds to J_w^1 . $\lambda^{N_{\mathcal{L}}}$ stands for the scaling caused by SCET_I Lagrangian. As a example, if we consider A_w is induced by the time-product $T[J_w^0, \mathcal{L}_{\xi\xi}^2, \mathcal{L}_{\xi q}^1]$, then we have $N_{\mathcal{L}} = 3$.

If we integrating out the DOFs $\sim \sqrt{m_b \Lambda_H}$, then the SCET_{II} are matched onto. According to Ref. [11], within SCET_{II}, the power counting for A_w is $\eta^{(N_J + N_{\mathcal{L}})/2 + N_{uc}}(N_{uc} \geq 0)$. N_{uc} is caused by lowering the off-shellness of the un-contracted collinear fields.

In this way, the leading contributions of A_w in η can be picked out.

1. Case of $N_J = 0, N_{\mathcal{L}} = 0$. Here we show that this kind of amplitudes do not contribute to the $B_c \rightarrow M_1 M_2$ processes. As to $B_c \rightarrow M_1 M_2$ decays, the final mesons involve even $n(\bar{n})$ -collinear quarks. However, as shown in Eq. (2), there is odd $n(\bar{n})$ -collinear quark field. No matter how many $\mathcal{L}_{c\bar{q}}^0$ and $\mathcal{L}_{\xi\xi}^0$ s are contracted with J_w^0 , there are

still odd final $n(\bar{n})$ -collinear quark fields. Therefore, the $B_c \rightarrow M_1 M_2$ processes do not include this kind of amplitudes.

2. Case of $N_J = 1, N_{\mathcal{L}} = 0$. Although there are even $n(\bar{n})$ -collinear quarks in J_w^1 , $B_c \rightarrow M_1 M_2$ transition still receives no contributions from this case. This is because the $n(\bar{n})$ DOF in J_w^1 is color-octet. In the leading SCET_I Lagrangian, namely, $N_{\mathcal{L}} = 0$, the n collinear DOFs decouple from the \bar{n} and ultra-soft ones. Thus, the final $n(\bar{n})$ fields are all generated originally from $B_{n,\omega}^{\perp\mu}$ in J_w^1 , which makes the final $n(\bar{n})$ meson color-octet. So the $B_c \rightarrow M_1 M_2$ decays do not contain the amplitudes for this case.
3. Case of $N_J = 0, N_{\mathcal{L}} = 1$. This case is similar to the $N_J = 0, N_{\mathcal{L}} = 0$ one, which also produces odd $n(\bar{n})$ -collinear quarks. Thus, there is no overlapping amplitude for the $B_c \rightarrow M_1 M_2$ transitions.
4. Case of $N_J = 2, N_{\mathcal{L}} = 0$. J_w^{2B} will contribute to $B_c \rightarrow M_1 M_2$ decays. J_w^{2A} contributes only for the isosinglet final states, such as $\eta, \eta'(958)$ mesons. Their typical diagrams are plotted in Figs. 1 (a,b).
5. Case of $N_J = 0, N_{\mathcal{L}} = 2$. In order to produce even $n(\bar{n})$ -collinear quarks, only $T[J_w^0, \mathcal{L}_{\xi n q}^1, \mathcal{L}_{\xi \bar{n} q}^1]$ is possible. But in this time-product, the number of $iD_{n(\bar{n})}^{\perp}$ is odd, which introduces extra suppressions from N_{uc} . In this case, $N_{uc} \geq 1$. Therefore, at the leading order in η , the amplitudes for $N_J = 0, N_{\mathcal{L}} = 2$ do not contribute.
6. Case of $N_J = 1, N_{\mathcal{L}} = 1$. In this case, the product $T[J_w^1, \mathcal{L}_{\xi q}^1]$ will not contribute, since it does not produce the even $n(\bar{n})$ -collinear quarks. But the products $T[J_w^1, \mathcal{L}_{\xi \xi}^1]$ and $T[J_w^1, \mathcal{L}_{cg}^1]$ do. The examples of these two products are illustrated in Figs. 1 (c,d).

In summary, the operators $J_w^{2A}, J_w^{2B}, T[J_w^1, \mathcal{L}_{\xi q}^1]$ and $T[J_w^1, \mathcal{L}_{cg}^1]$ contribute to the $B_c \rightarrow M_1 M_2$ processes in the leading order in η . The according transition amplitudes are

$$\begin{aligned}
A_{wA}^2 &= \langle M_1 M_2 | J_w^{2A}(0) | B_c^- \rangle, \\
A_{wB}^2 &= \langle M_1 M_2 | J_w^{2B}(0) | B_c^- \rangle, \\
A_{wC}^2 &= \langle M_1 M_2 | \int dx T[J_w^1(0), \mathcal{L}_{\xi \xi}^1(x)] | B_c^- \rangle, \\
A_{wD}^2 &= \langle M_1 M_2 | \int dx T[J_w^1(0), \mathcal{L}_{cg}^1(x)] | B_c^- \rangle.
\end{aligned} \tag{4}$$

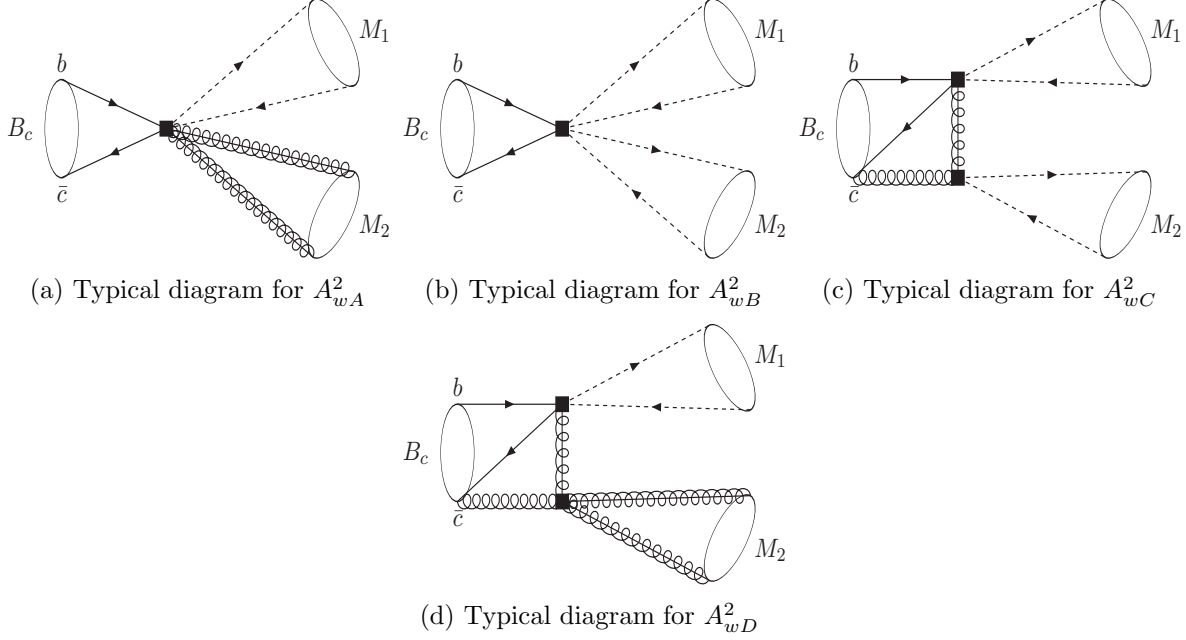


FIG. 1: Typical diagrams for A_{wA}^2 , A_{wB}^2 , A_{wC}^2 and A_{wD}^2 . The solid lines stand for the initial $b(\bar{c})$ quarks, while the dash lines denote the final collinear quarks. A spring is the (ultra-)soft gluon, but the spring with a line though it represents the collinear gluon. Figs. (a,d) contribute only to the isosinglet final meson, such η , $\eta'(958)$.

Consider that in the leading SCET_I Lagrangian the collinear fields decouple from the ultra-soft fields. Therefore, we have

$$\begin{aligned}
A_{wA}^2 &= \int d\omega_1 d\omega_2 d\omega_3 d\omega_4 C_w^{2A}(\omega_1, \omega_2, \omega_3, \omega_4) \langle 0 | \chi_{\bar{c}}^\dagger \Gamma_{\mu\nu}^{2A} \psi_b | B_c^- \rangle \langle M_1 | \bar{q}'_{\bar{n}, \omega_2} \Gamma_{\bar{n}} q_{\bar{n}, \omega_3} | 0 \rangle \\
&\quad \langle M_2 | \text{Tr}[B_{n, \omega_1}^{\perp\mu} B_{n, \omega_4}^{\perp\nu}] | 0 \rangle, \\
A_{wB}^2 &= \int d\omega_1 d\omega_2 d\omega_3 d\omega_4 C_w^{2B}(\omega_1, \omega_2, \omega_3, \omega_4) \langle 0 | \chi_{\bar{c}}^\dagger \Gamma^{2B} \psi_b | B_c^- \rangle \langle M_1 | \bar{q}'_{\bar{n}, \omega_2} \Gamma_{\bar{n}} q_{\bar{n}, \omega_3} | 0 \rangle \\
&\quad \langle M_2 | \bar{q}'_{n, \omega_1} \Gamma_n q_{n, \omega_4} | 0 \rangle.
\end{aligned} \tag{5}$$

However, there are interactions between the collinear and ultra-soft fields in $\mathcal{L}_{\xi\xi}^1$ and \mathcal{L}_{cg}^1 . Thus, we have

$$\begin{aligned}
A_{wC}^2 &= \int dx d\omega d\omega_2 d\omega_3 C_w^1(\omega, \omega_2, \omega_3) \langle M_2 | T \left[\left(\chi_{\bar{c}}^\dagger \Gamma_\mu^1 \psi_b B_{n, \omega}^{\perp\mu} \right) (0), \mathcal{L}_{\xi\xi}^1(x) \right] | B_c^- \rangle \langle M_1 | \left(\bar{q}'_{\bar{n}, \omega_2} \Gamma_{\bar{n}} q_{\bar{n}, \omega_3} \right) | 0 \rangle, \\
A_{wD}^2 &= \int dx d\omega d\omega_2 d\omega_3 C_w^1(\omega, \omega_2, \omega_3) \langle M_2 | T \left[\left(\chi_{\bar{c}}^\dagger \Gamma_\mu^1 \psi_b B_{n, \omega}^{\perp\mu} \right) (0), \mathcal{L}_{cg}^1(x) \right] | B_c^- \rangle \langle M_1 | \left(\bar{q}'_{\bar{n}, \omega_2} \Gamma_{\bar{n}} q_{\bar{n}, \omega_3} \right) | 0 \rangle.
\end{aligned} \tag{6}$$

The typical diagrams of A_{wA}^2 , A_{wB}^2 , A_{wC}^2 and A_{wD}^2 are illustrated in Fig. 1.

C. The analysis of A_{wB}^2

In the last subsection, we prove the factorization formulae of A_{wA}^2 , A_{wB}^2 , A_{wC}^2 and A_{wD}^2 . Here we lay stress on the calculations of A_{wB}^2 . The analysis of A_{wA}^2 can be performed in a similar manner. The estimations of A_{wC}^2 and A_{wD}^2 involve the non-factorizable matrix elements $\langle M_2 | T \left[\left(\chi_{\bar{c}}^\dagger \Gamma_\mu^1 \psi_b B_{n,\omega''}^{\perp\mu} \right) (0), \mathcal{L}_{\xi\xi}^1(x) \right] | B_c^- \rangle$ and $\langle M_2 | T \left[\left(\chi_{\bar{c}}^\dagger \Gamma_\mu^1 \psi_b B_{n,\omega''}^{\perp\mu} \right) (0), \mathcal{L}_{cg}^1(x) \right] | B_c^- \rangle$. We expect them to be determined from the future experimental data or the non-perturbative method.

For the amplitude A_{wB}^2 , as shown in Eq. (5), the hadronic matrix elements $\langle 0 | \chi_{\bar{c}}^\dagger \Gamma^{2B} \psi_b | B_c^- \rangle$, $\langle M_1 | \bar{q}'_{\bar{n},\omega_2} \Gamma_{\bar{n}} q_{\bar{n},\omega_3} | 0 \rangle$ and $\langle M_2 | \bar{q}'_{n,\omega_1} \Gamma_n q_{n,\omega_4} | 0 \rangle$ are involved.

Considering that the B_c meson is dominated by the $^1S_0^{[1]}$ Fock state, the matrix Γ^{2B} should be I and the initial hadronic matrix element can be parameterized as

$$\langle 0 | \chi_{\bar{c}}^\dagger \psi_b | B_c^- \rangle = i f_{B_c} M_{B_c}, \quad (7)$$

where f_{B_c} is decay constant of the B_c meson.

As to the final hadronic matrix elements, the matrices Γ_n and $\Gamma_{\bar{n}}$ are involved. In general, they can be represented by the following basis

$$\{I, \gamma_5, \not{n}, \not{\bar{n}}, \gamma_\perp^\mu, \not{n}\gamma_5, \not{\bar{n}}\gamma_5, \gamma_\perp^\mu\gamma_5, \not{n}\gamma_\perp^\mu, \not{\bar{n}}\gamma_\perp^\mu, (\not{n} \not{\bar{n}} - 2)\}.$$

If the properties of the SCET_I fields $\frac{n'\bar{n}'}{4}q_{n,\omega_i} = q_{n,\omega_i}$ and $\frac{\bar{n}'n'}{4}q_{\bar{n},\omega_i} = q_{\bar{n},\omega_i}$ are considered, only the set of matrices $\Gamma_n = \not{n}P_L$ and $\Gamma_{\bar{n}} = \not{\bar{n}}P_L$ contribute. (The constructions of these local six-quark operators are discussed detailedly in Ref. [17]. Here we directly use their results.)

Therefore, we have $\langle M_1 | \bar{q}'_{\bar{n},\omega_2} \not{n}P_L q_{\bar{n},\omega_3} | 0 \rangle$ and $\langle M_2 | \bar{q}'_{n,\omega_1} \not{\bar{n}}P_L q_{n,\omega_4} | 0 \rangle$. According to Ref. [15], these two hadronic matrix elements are just the conventional light cone wave functions in the momentum space. Based on Ref. [18], we have

$$\begin{aligned} \langle P(p) | \bar{q}_{n,\omega_q} \not{\bar{n}}P_L q'_{n,\omega_{q'}} | 0 \rangle &= \frac{-i f_{Pp} \cdot \bar{n}}{2} \int_0^1 dx \delta(xp \cdot \bar{n} - \omega_q) \delta(\bar{x}p \cdot \bar{n} + \omega_{q'}) \phi_P, \\ \langle V(p) | \bar{q}_{n,\omega_q} \not{\bar{n}}P_L q'_{n,\omega_{q'}} | 0 \rangle &= \frac{-i f_{Vp} \cdot \bar{n}}{2} \int_0^1 dx \delta(xp \cdot \bar{n} - \omega_q) \delta(\bar{x}p \cdot \bar{n} + \omega_{q'}) \phi_V, \end{aligned} \quad (8)$$

where $\bar{x} = 1 - x$. Usually, $\phi_{P(V)}$ can be expanded in the Gegenbauer polynomials [19]

$$\phi_{P(V)} = 6x(1-x) \left[1 + \sum_{n=1}^{\infty} a_{P(V)}^n C_n^{3/2}(2x-1) \right], \quad (9)$$

where $a_{P(V)}^n$ s are the Gegenbauer moments, which can be obtained from lattice simulations [20, 21]. $C_n^{3/2}(u)$ s are the Gegenbauer polynomials. In our numerical calculations, we truncate this expansion at $n = 2$, using $C_1(u) = 3u$ and $C_2 = \frac{3}{2}(5u^2 - 1)$.

Plugging Eqs. (7-8) into Eq. (5), A_{wB}^2 can be re-written as

$$A_{wB}^2 = \frac{f_{B_c} f_{M_1} f_{M_2}}{27} \int_0^1 dx dy C_w^1(x, y) \phi_{M_1}(x) \phi_{M_2}(y). \quad (10)$$

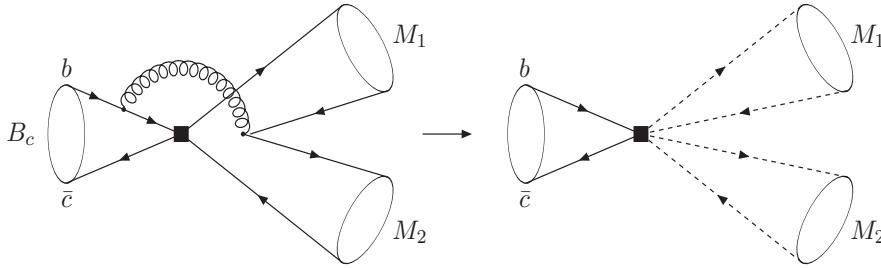


FIG. 2: Matching procedure for A_{wB}^2 in QCD (left diagram) and SCET (right diagram).

Matching at tree level, as shown in Fig. 2, we have

$$C_w^1(x, y) = \frac{4\pi G_F \alpha_s(m_b) C_2 V_{cb} V_{uq}^*}{\sqrt{2} y (\bar{x}y - \alpha_1 \bar{x} - \alpha_1 y + i\epsilon)}, \quad (11)$$

where $\alpha_1 = m_b/M_{B_c}$. This result is in agreement with the one in Ref. [1]. If we take $\alpha_1 \rightarrow 1$, Eq. (11) also agree with the results in Refs. [17, 19].

D. The Leading contributions of A_c

In this part, we turn to analyzing the leading A_c in η . A_c s are induced by one J_w and at least one J_c . From the SCET power counting rules, at the leading order in η , A_c^0 is mediated by $T[J_w^0, J_c^0]$. The expression of J_w^0 has been given in Eq. (2). For J_c^0 , at the tree level

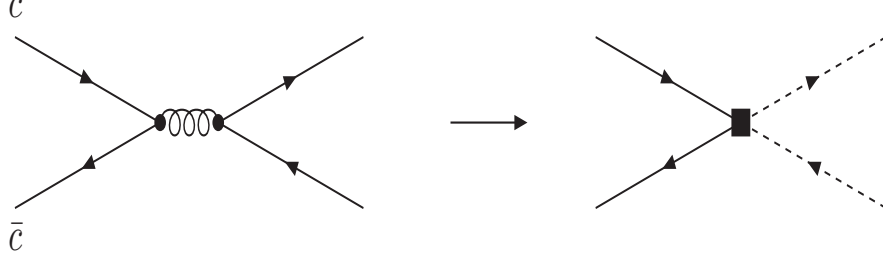


FIG. 3: Matching procedure for J_c^0 in QCD (left diagram) and SCET (right diagram).

matching, as shown in Fig. 3, we have

$$J_c^0 = \int d\omega_1 d\omega_3 \left[D_1(\chi_{\bar{c}}^\dagger \sigma_\perp^\mu \psi_c)(\bar{q}_{n,\omega_1} \gamma_{\perp\mu} q_{\bar{n},\omega_3}) + D_2(\chi_{\bar{c}\beta}^\dagger \sigma_\perp^\mu \psi_{c,\alpha})(\bar{q}_{n,\omega_1\alpha} \gamma_{\perp\mu} q_{\bar{n},\omega_3\beta}) \right]. \quad (12)$$

Here $D_1 = \frac{2\pi\alpha_s(m_b)}{3\omega_1\omega_3}$ and $D_2 = \frac{-2\pi\alpha_s(m_b)}{\omega_1\omega_3}$.

The factorization properties of SCET yield that A_c^0 can be re-written as

$$A_c^0 \propto \sum_{i,j} \int dz d\omega_1 d\omega_2 d\omega_3 d\omega_4 C_w^{0i} D_j e^{-i(\omega_1 - \omega_3)z} \langle 0 | T \left\{ \left[\chi_{\bar{c}}^\dagger \Gamma_A^{01} \psi_b \right] (0), \left[\chi_{\bar{c}}^\dagger \sigma_\perp^\mu \psi_c \right] (z) \right\} | B_c^- \rangle \langle M_1 | \bar{q}'_{\bar{n},\omega_2} \Gamma_{\bar{n}} q_{\bar{n},\omega_3} | 0 \rangle \langle M_2 | \bar{q}'_{n,\omega_1} \Gamma_n q_{n,\omega_4} | 0 \rangle. \quad (13)$$

In Eq. (13), the color indices are implicit for readability. The example of this amplitude is illustrated in Fig. 4.

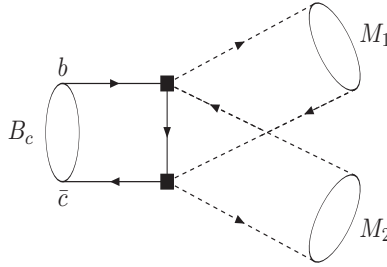


FIG. 4: Typical diagrams for A_c^0 .

Here we interpret the first hadronic term in Eq. (13) as the non-perturbative soft functions. This is because that the soft gluons may be exchanged between the produced c quark and the initial constituent $b(\bar{c})$ quark.

In order to see this, we approximatively consider $\omega_2 = -\omega_3 = \omega_1 = -\omega_4 = M_{B_c}/2$.

In this way, the c quark produced by J_w^0 moves non-relativistically and is almost on-shell. When this c quark and the initial constituent \bar{c} quark are annihilated by J_c^0 , it is observed that $(\tilde{P}_c + P_{\bar{c}})^2 \sim M_{J/\psi}^2$. (\tilde{P}_c denotes the momentum of the propagated c quark, while $P_{\bar{c}}$ stands for the initial constituent \bar{c} quark.) Therefore, it is reasonable to expect soft gluons exchanged between the propagated c and the initial partons.

Actually, this situation is not unique in the analysis of SCET. In the $B \rightarrow M_1 M_2$ processes, there are long-distance charming penguins [22], in which soft gluons are also exchanged among the produced c quarks, the spectator quark and the initial b quark.

III. NUMERICAL RESULTS AND THE DISCUSSIONS

In this part, we present the numerical results and phenomenal analysis. In Sec. III A, the inputs in the calculations are introduced. Within Sec. III B, the numerical results are shown.

A. Inputs in calculations

The masses and lifetimes of the involved mesons are presented in Table. 1. The mass for b quark is taken as $m_b = 4.8$ GeV [23], while the mass of c quark is used as $m_c = 1.6$ GeV [23].

TABLE II: Masses and lifetimes.

Meson	B_c	π	K	ρ	K^*
Mass [23]	6.3 GeV	0.14 GeV	0.49 GeV	0.77 GeV	0.89 GeV
Lifetime [23]	0.51×10^{-12} s				

In Eq. (1) and Eq. (11), α_s and the Wilson coefficients C_1 and C_2 are involved. Here we take $\alpha_s(m_b) = 0.22$, $C_1 = 1.078$ and $C_2 = -0.184$ [12].

In Eqs. (7-8), the decay constants $f_{B_c, P, V}$ and the Gegenbauer moments $a_{1,2}$ are involved. According to Ref. [24], we employ $f_{B_c} = 0.322$ GeV. The other inputs are summerized in Table. 2.

TABLE III: Decay constants and the Gegenbauer moments for the light mesons.

Meson	π	K	Meson	ρ	K^*
f_M [23]	0.130 GeV	0.156 GeV	f_M [23]	0.208 GeV	0.217 GeV
a_1 [20, 21]	-	0.0583	a_1^{\parallel} [21]	-	0.0716
a_2 [20, 21]	0.136	0.175	a_2^{\parallel} [21]	0.204	0.145

B. Numerical results

Here we only show the numerical results of A_{wB}^2 . A_{wA}^2 does not contribute to the open flavor final states, while the evaluations of A_c^0 , A_{wC}^2 and A_{wD}^2 involve the non-perturbative hadronic matrix elements. We leave the calculations on A_c^0 , A_{wC}^2 and A_{wD}^2 to the future work.

TABLE IV: Numerical results of A_{wB}^2 in 10^{-10} GeV.

	Results
$A_{wB}^2(B_c^- \rightarrow K^- K^0)$	-4.50
$A_{wB}^2(B_c^- \rightarrow K^{*-} K^0)$	-5.94
$A_{wB}^2(B_c^- \rightarrow K^- K^{*0})$	-6.27
$A_{wB}^2(B_c^- \rightarrow \pi^- \bar{K}^0)$	-0.89
$A_{wB}^2(B_c^- \rightarrow \pi^- \bar{K}^{*0})$	-1.24

A_{wB}^2 can be obtained from Eqs. (10-11). The numerical results are listed in Table. IV. First, from Table. IV, all of the A_{wB} results are real. This also happens in the local annihilation amplitudes of the $B \rightarrow M_1 M_2$ decays [17]. Second, one may note that $A_{wB}^2(B_c^- \rightarrow K^- K^0)$ are comparable with the ones of the $B_c^- \rightarrow K^{*-} K^0$ and $B_c^- \rightarrow K^- K^{*0}$ processes, but much larger than the $B_c^- \rightarrow \pi^- \bar{K}^0$ and $B_c^- \rightarrow \pi^- \bar{K}^{*0}$ cases. This is caused by the suppressed CKM matrix, namely, $V_{us}/V_{ud} \sim \lambda = 0.22$ [23]. Third, although our expression of A_{wB}^2 is formally identical to the one in Ref. [1], the results in Table. IV are different from them. In Ref. [1], the integration in Eq. (11) is done with expanding the parameter α_1 and take the asymptotic wave functions. However, in this work, the calculations are performed without these approximations.

IV. CONCLUSION

In this paper, we investigate the $B_c \rightarrow M_1 M_2$ decays with the framework of (p)NRQCD+SCET. Our analysis shows that the leading amplitudes for $B_c \rightarrow M_1 M_2$ processes include A_{wA}^2 , A_{wB}^2 , A_{wC}^2 , A_{wD}^2 and A_c^0 .

As to A_{wA}^2 and A_{wB}^2 , from the SCET properties, they can be factorized into the following form

$$H \otimes \Phi_{B_c} \otimes \Phi_{\bar{n}} \otimes \Phi_n. \quad (14)$$

Here H denotes the hard kernel, while Φ_{B_c} and $\Phi_{n(\bar{n})}$ stand for the initial and final wave functions, respectively. This factorization formulae is in agreement with the PQCD [2, 3] and QCDF [1] results. And our result on A_{wB}^2 is formally identical to Ref. [1].

But for A_{wC}^2 , A_{wD}^2 and A_c^0 , the situations are different. The amplitude A_c^0 includes the initial soft functions, while the ones A_{wC}^2 and A_{wD}^2 involve the lagrangian $\mathcal{L}_{\xi\xi}^1$ and \mathcal{L}_{cg}^1 , where the collinear fields are tangled with ultra-soft gluons. Therefore, we expect the amplitudes A_{wC}^2 , A_{wD}^2 and A_c^0 can not be expressed as the form in Eq. (14).

Acknowledgments

This work was supported in part by the National Natural Science Foundation of China (NSFC) under Grant No. 11575048, No. 11405037 and No. 11505039. T.Wang was also supported by PIRS of HIT No.B201506.

Appendix A: Details on the A_{wB}^2 calculation

In this part, we introduce the details on the A_{wB}^2 calculation. From Eq. (10), it is observed that the numerator of the integrand is a polynomial of x and y . Hence, we can expand A_{wB}^2 in terms of $I(m, n)$ s, namely, $A_{wB}^2 = \sum_{m,n=0}^{\infty} \mathcal{B}(m, n) I(m, n)$. $\mathcal{B}(m, n)$ is the according parameter, while the elemental integration $I(m, n)$ ($m, n \geq 0$) is defined as

$$I(m, n) = \int_0^1 dx dy \frac{x^m y^n}{xy - \alpha_1 x - \alpha_1 y + i\epsilon}. \quad (\text{A1})$$

From Eq. (A1), we see $I(m, n) = I(n, m)$. Hence, in the following paragraphs only $I(m, n)$ ($m \geq n \geq 0$) is introduced. The case for $n > m > 0$ can be obtained from the symmetries.

For the term $I(0, 0)$, we have

$$I(0, 0) = -\text{Li}_2 \left(-\frac{(1 - \alpha_1)^2}{-\alpha_1^2 + i\epsilon} \right) + \text{Li}_2 \left(\frac{(1 - \alpha_1)\alpha_1}{-\alpha_1^2 + i\epsilon} \right) + \text{Li}_2 \left(-\frac{(-1 + \alpha_1)\alpha_1}{-\alpha_1^2 + i\epsilon} \right) - \text{Li}_2 \left(-\frac{\alpha_1^2}{-\alpha_1^2 + i\epsilon} \right). \quad (\text{A2})$$

It seems that the analysis from the Landau equations [25, 26] implies the end-point singularities in $I(0, 0)$. But a careful study shows that those singularities are not in the principal sheet. Hence, $I(0, 0)$ is finite. Compared with other $I(m, n)$ s, it is observed that $I(0, 0)$ is the most singular term. Thus, all $I(m, n)$ s are also finite. This conclusion agrees with Ref. [1].

For the term $I(m, 0)$ ($m \geq 1$), we have

$$I(m, 0) = \alpha^n I(0, 0) + \int_{-\alpha_1}^{1-\alpha_1} du \sum_{i=0}^{n-1} (C_n^i u^{n-1-i} \alpha_1^i) [\text{Log}(u - \alpha_1 u - \alpha_1^2 + i\epsilon) - \text{Log}(-\alpha_1 u - \alpha_1^2 + i\epsilon)], \quad (\text{A3})$$

where C_n^i is the binomial coefficient.

As to the term $I(m, n)$ ($m \geq n \geq 1$), it is

$$I(m, n) = \sum_{j=0}^n C_n^j \alpha_1^n I(n - j, m - n + j) + \int_0^1 dx dy \sum_{i=0}^{n-1} C_n^i y^{m-n} (\alpha_1 x + \alpha_1 y)^i (xy - \alpha_1 x - \alpha_1 y)^{n-1-i} \quad (\text{A4})$$

We can evaluate this equation inductively, because the powers of $I(n-j, m-n+j)$ s are no more than m . For instance, $I(1, 1) = 2\alpha_1 I(1, 0) + 1$, where $I(1, 0)$ can be computed from Eq. (A3).

Consequently, based on Eqs. (A2-A4), all of $I(m, n)$ s can be evaluated. The use of these $I(m, n)$ s are quite general. They can not only be employed to calculate Eq. (10), if we make proper replacements of α_1 , they are also useful in the calculations of Ref. [1].

-
- [1] S. Descotes-Genon, J. He, E. Kou and P. Robbe, Phys. Rev. D **80**, 114031 (2009).
 - [2] X. Liu, Z. J. Xiao and C. D. Lu, Phys. Rev. D **81**, 014022 (2010).
 - [3] Y. L. Yang, J. F. Sun and N. Wang, Phys. Rev. D **81**, 074012 (2010).
 - [4] G. T. Bodwin, E. Braaten and G. P. Lepage, Phys. Rev. D **51** (1995) 1125 [Phys. Rev. D **55** (1997) 5853] [hep-ph/9407339].
 - [5] M. E. Luke, A. V. Manohar and I. Z. Rothstein, Phys. Rev. D **61** (2000) 074025 [hep-ph/9910209].
 - [6] C. W. Bauer, S. Fleming and M. E. Luke, Phys. Rev. D **63**, 014006 (2000) [hep-ph/0005275].
 - [7] C. W. Bauer, S. Fleming, D. Pirjol and I. W. Stewart, Phys. Rev. D **63**, 114020 (2001) [hep-ph/0011336].
 - [8] C. W. Bauer and I. W. Stewart, Phys. Lett. B **516**, 134 (2001) [hep-ph/0107001].
 - [9] C. W. Bauer, D. Pirjol and I. W. Stewart, Phys. Rev. D **65** (2002) 054022 [hep-ph/0109045].
 - [10] C. W. Bauer, D. Pirjol and I. W. Stewart, Phys. Rev. D **67**, 071502 (2003) [hep-ph/0211069].
 - [11] C. W. Bauer, D. Pirjol and I. W. Stewart, Phys. Rev. D **68**, 034021 (2003) [hep-ph/0303156].
 - [12] G. Buchalla, A. J. Buras and M. E. Lautenbacher, Rev. Mod. Phys. **68**, 1125 (1996) [hep-ph/9512380].
 - [13] M. Beneke and V. A. Smirnov, Nucl. Phys. B **522**, 321 (1998) [hep-ph/9711391].
 - [14] W. Wang and R. L. Zhu, Eur. Phys. J. C **75**, no. 8, 360 (2015) [arXiv:1501.04493 [hep-ph]].
 - [15] C. W. Bauer, D. Pirjol and I. W. Stewart, Phys. Rev. Lett. **87**, 201806 (2001) [hep-ph/0107002].
 - [16] D. Pirjol and I. W. Stewart, Phys. Rev. D **67**, 094005 (2003) [Phys. Rev. D **69**, 019903 (2004)] [hep-ph/0211251].
 - [17] C. M. Arnesen, Z. Ligeti, I. Z. Rothstein and I. W. Stewart, Phys. Rev. D **77**, 054006 (2008)

- [hep-ph/0607001].
- [18] M. Beneke and T. Feldmann, Nucl. Phys. B **592**, 3 (2001) [hep-ph/0008255].
 - [19] M. Beneke, G. Buchalla, M. Neubert and C. T. Sachrajda, Nucl. Phys. B **606**, 245 (2001) [hep-ph/0104110].
 - [20] V. M. Braun, S. Collins, M. G?ckeler, P. Prez-Rubio, A. Sch?fer, R. W. Schiel and A. Sternbeck, arXiv:1510.07429 [hep-lat].
 - [21] R. Arthur, P. A. Boyle, D. Brommel, M. A. Donnellan, J. M. Flynn, A. Juttner, T. D. Rae and C. T. C. Sachrajda, Phys. Rev. D **83**, 074505 (2011) [arXiv:1011.5906 [hep-lat]].
 - [22] C. W. Bauer, D. Pirjol, I. Z. Rothstein and I. W. Stewart, Phys. Rev. D **70**, 054015 (2004) [hep-ph/0401188].
 - [23] K. A. Olive *et al.* [Particle Data Group Collaboration], Chin. Phys. C **38** (2014) 090001.
 - [24] G. Cvetič, C. S. Kim, G. L. Wang and W. Namgung, Phys. Lett. B **596**, 84 (2004) [hep-ph/0405112].
 - [25] L. D. Landau, Nucl. Phys. **13**, 181 (1959).
 - [26] L. D. Landau, “On analytic properties of vertex parts in quantum field theory,”